

Microstructural Characterization of Fluoropolymers via Two-Dimensional $^1\text{H}/^{19}\text{F}/^{13}\text{C}$ Triple-Resonance NMR Techniques

Lan Li, Dale G. Ray III, and Peter L. Rinaldi*

Knight Chemical Laboratory, Department of Chemistry, The University of Akron, Akron, Ohio 44325-3601

Hsin-Ta Wang and H. James Harwood

The Maurice Morton Institute of Polymer Science, Department of Polymer Science, The University of Akron, Akron, Ohio 44325-3909

Received January 2, 1996; Revised Manuscript Received March 28, 1996

ABSTRACT: This paper demonstrates the utility of $^{19}\text{F}/^{13}\text{C}$ chemical shift correlation 2D-NMR experiments for characterizing fluoropolymers. $^{19}\text{F}\{^{13}\text{C}\}$ HMQC and HMBC (with simultaneous ^1H decoupling) provide greatly simplified spectra with almost no loss of sensitivity compared to the routinely used $^1\text{H}\{^{13}\text{C}\}$ heteronuclear multiple-quantum coherence (HMQC) and heteronuclear multiple-bond connectivity (HMBC) NMR experiments and exploit the large chemical shift dispersion of both ^{13}C and ^{19}F nuclei to achieve tremendous spectral dispersion. The utility of these methods in obtaining resonance assignments is illustrated using spectra of poly(1-chloro-1-fluoroethylene-*co*-isobutylene).

Introduction

Obtaining complete NMR resonance assignments for copolymers is usually complicated by overlapping lines arising from the diverse range of microenvironments present. Quite often the characterization of copolymers using 1D ^1H or ^{13}C NMR experiments requires combinations of several techniques and examination of a series of copolymers prepared for a range of monomer feed compositions. These include correlations of resonance areas with calculated sequence distribution information, the development of empirical chemical shift rules, and the investigation of the spectra of model compounds and of copolymers prepared from isotopically labeled monomers. 2D NMR techniques, especially inverse detected 2D heteronuclear shift correlation experiments, offer the opportunity to simplify the task since they enable one to obtain the configurational and sequence assignments of polymers by using NMR experiments alone. These experiments provide much more information than 1D experiments because they disperse resonances into a second dimension, enabling the resolution of signals from many additional species. Additionally, they provide greatly enhanced sensitivity, enabling the detection of species which are present at very low concentrations, and they provide correlations which indicate atomic connectivities.

^1H -detected heteronuclear multiple-quantum coherence (HMQC)^{1,2} and heteronuclear multiple-bond connectivity (HMBC)³ experiments have been routinely used for the characterization of biological molecules. Recently, these experiments have also become effective methods for investigating the microstructures of polymers. HMQC provides the same information contained in the heteronuclear shift correlation (HETCOR)^{4–6} experiment but has a theoretical 64-fold sensitivity gain ($\gamma^3_{\text{H}}/\gamma^3_{\text{C}}$, where γ is the magnetogyric ratio of a nucleus), compared to the experiments involving direct detection of ^{13}C . HMBC is the long-range version of HMQC, and it provides correlations between the resonances of ^1H and ^{13}C nuclei which have two- and three-bond J couplings. Although these experiments are commonly

performed with ^1H and ^{13}C nuclei, any two nuclei exhibiting resolvable couplings can be used.

The $^{19}\text{F}/^{13}\text{C}$ spin pair is an ideal system to use in extending the application of these methods. ^{19}F NMR has sensitivity comparable to that of ^1H , since the ^{19}F isotope has 100% natural abundance, a spin $I = 1/2$, and a large γ . Substitution of ^{19}F for ^1H in 2D-HMQC and HMBC experiments has the additional advantage of a much larger chemical shift range, larger coupling constants (especially two- and three-bond couplings), and better defined ranges for two-, three-, and four-bond C–F couplings. These characteristics make $^{19}\text{F}\{^{13}\text{C}\}$ HMQC and HMBC experiments ideally suited for the characterization of fluoropolymers.⁷

The 1D NMR spectra of fluorine-containing copolymers are usually very complex.⁸ Note only are there numerous possibilities of monomer sequences and stereosequences, but the spectra are also complicated by the presence of couplings with ^{19}F . Figure 1 shows possible E-centered pentad structures of poly(1-chloro-1-fluoroethylene-*co*-isobutylene), P(CFE–IB), where E and I represent 1-chloro-1-fluoroethylene and isobutylene monomer units, respectively, while m and r represent the meso and racemic configurations that involve two adjacent E monomer units. In this paper, we show that the 2D $^{19}\text{F}\{^{13}\text{C}\}$ HMQC and HMBC experiments, obtained with simultaneous ^1H decoupling, provide simplified, well-dispersed spectra that take advantage of both ^{19}F and ^{13}C large chemical shift ranges, making nearly complete resonance assignments possible. In a subsequent paper, we will report the results of quantitative studies on the ^1H , ^{13}C , and ^{19}F spectra of P(CFE–IB) samples that are based in part on the ^{13}C and ^{19}F assignments made herein.

Experimental Section

Materials. Poly(1-chloro-1-fluoroethylene-*co*-isobutylene) was synthesized in less than 10% conversion by bulk polymerization at 46 °C, using azobis(1,4-dimethyl-4-methoxyvaleronitrile) as the initiator. The two samples used in this work, designated P(CFE–IB) 3:1 and P(CFE–IB) 1:1, respectively, were obtained from monomer feed ratios of 3:1 and 1:1 of 1-chloro-1-fluoroethylene (E) and isobutylene (I). They contained 65 and 43 mol % E units, respectively, based on comparison of the CH_3 and CH_2 resonances areas obtained in the ^1H spectra.

* Abstract published in *Advance ACS Abstracts*, May 15, 1996.

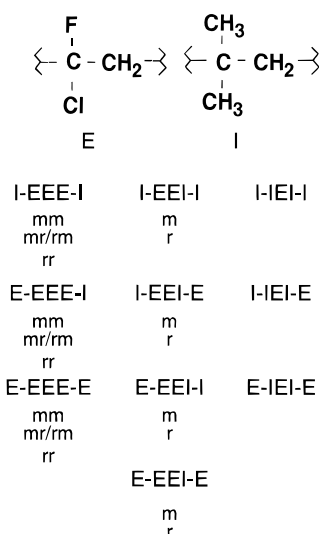


Figure 1. Possible pentad structures for P(CFE-IB), where E represents a 1-chloro-1-fluoroethylene unit and I represents an isobutylene unit. The possible stereosequences for the central triads are listed below the pentad monomer sequences.

NMR Measurements. The NMR spectra were collected at 30 °C on a Varian Unityplus 600 MHz NMR spectrometer equipped with three broad-band rf channels and an indirect detection triple-resonance probe from Nalorac Cryogenics with channels pretuned to the ^1H , ^{19}F , ^{13}C , and ^2H (lock) frequencies. CDCl_3 was used as the solvent as well as the internal reference for ^1H and ^{13}C chemical shifts; CFCl_3 was used as an external reference ($\delta_{19\text{F}} = 0$ ppm) for ^{19}F chemical shifts. The 2D spectra were acquired using phase-sensitive detection according to the method of States et al.⁹

The $^{19}\text{F}\{^{13}\text{C}\}$ HMQC spectra were obtained at 564 MHz using a 0.02 s acquisition time (with ^{13}C Garp decoupling), a 0.2 s BIRD^{3,10} of nulling decay, a 0.5 s relaxation delay, spectral windows of 22 523 Hz in F_2 and 10 000 Hz in F_1 , a 21.5 μs 90° ^{19}F pulse, and a 16.0 μs ^{13}C 90° pulse. A 2D matrix of 1024 (512 \times 2) increments was obtained with averaging of 64 transients for each t_1 increment. Waltz-16 ^1H decoupling was used throughout the experiments.

The $^{19}\text{F}\{^{13}\text{C}\}$ HMBC spectra was obtained at 564 MHz using a 0.04 s acquisition time, a 19 ms τ delay, a 0.5 s relaxation delay, spectral windows of 22 523 Hz in F_2 and 19 608 Hz in F_1 , a 21.5 μs 90° ^{19}F pulse, and a 16.0 μs ^{13}C 90° pulse. A 2D matrix of 1024 (512 \times 2) increments was obtained with averaging of 64 transients for each t_1 increment. Waltz-16 ^1H decoupling was also used throughout these experiments.

All data were processed with Varian's VNMR software. Line broadening of 3 Hz and zero filling to 4 times the original data sized were used before Fourier transformation of the 1D data. The 2D-HMQC and HMBC data were processed with a shifted sinebell weighting function and zero filling to 4 times the number of points collected in the F_1 dimension and 2 times the number of points collected in the F_2 dimension.

Results and Discussion

1D NMR Spectra. Figure 2a shows the 1D ^{19}F spectrum of P(CFE-IB) 3:1. At least 12 groups of peaks are evident, indicating that the ^{19}F chemical shifts are extremely sensitive to differences in microstructure. The broad lines are not due to relaxation but are the result of a large number of structures present in the sample and the presence of H-F and F-F J couplings.

Figure 2b shows the ^{13}C spectrum of P(CFE-IB) 3:1 obtained with both ^1H and ^{19}F decoupling. The downfield groups of resonances (108–117 ppm) arise from fluorinated carbons. The complexity in this region is reflective of the complex mixture of comonomer sequences present within the polymer. Since the ^{13}C spectrum of poly(1-chloro-1-fluoroethylene), P(CFE),

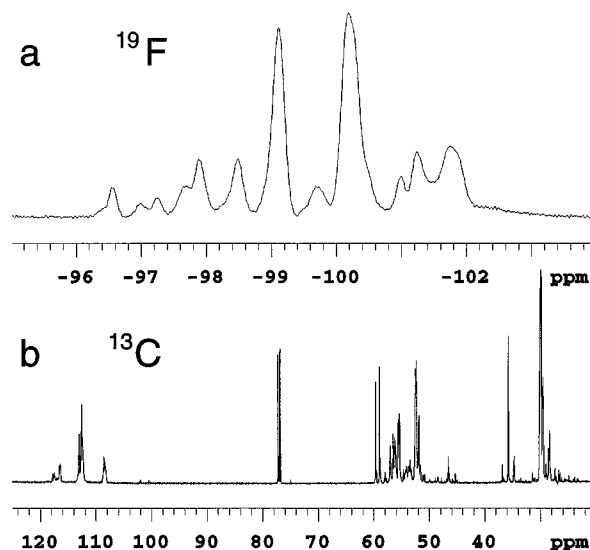


Figure 2. (a) ^{19}F and (b) ^{13}C 1D-NMR spectra of P(CFE-IB) 3:1.

exhibits only a singlet at 108 ppm, the EEE, EEI, and IEI triad sequences can be assigned to the three groups of resonances in the 108.2–108.8, 112.0–113.3, and 115.8–116.8 ppm regions, respectively.¹¹ The 50–62 ppm region of the ^{13}C spectrum contains the methylene resonances of both monomer units and is relatively complex. The 35–38 ppm region and the 26–32 ppm region contain the quaternary and methyl ^{13}C resonances of isobutylene monomer units, respectively. It would be extremely difficult to assign the various resonances observed in the 1D spectra working with the individually. However, by investigating them in concert using 2D techniques, it is possible to assign the resonances in a systematic logical manner.

2D $^{19}\text{F}\{^{13}\text{C}\}$ HMQC NMR Spectra. Figures 3a and 4a show the ^{19}F -detected $^{19}\text{F}\{^{13}\text{C}\}$ HMQC spectra of P(CFE-IB) obtained from 3:1 and 1:1 E/I monomer feed ratios, respectively. Correlations between directly bound ^{19}F and ^{13}C atoms in $-\text{CF}(\text{Cl})-$ fragments are observed. The $^{19}\text{F}\{^{13}\text{C}\}$ HMQC spectrum makes advantageous use of both ^{19}F and ^{13}C spectral dispersion, permitting the resolution of over 30 different cross-peaks in Figure 3a. Three groups of cross-peaks in regions A, B, and C along the F_1 (^{13}C) dimension are observed. As explained in considering the 1D spectrum (Figure 2a), they correspond to EEE, EEI, and IEI triad structures, respectively. The relative complexity of these regions is consistent with the number of triad sequences expected. EEE triads have three stereogenic centers and should give the most complicated spectrum (region A); IEI triads do not contain multiple stereogenic centers and are expected to provide the simplest spectrum (region C). Each replacement of an E with an I monomer unit in an EEE triad to form EEI and IEI triads results in a progressive 4.0 ppm downfield shift of the $-\text{CF}(\text{Cl})-$ ^{13}C resonance and a progressive 2.0 ppm upfield shift of the ^{19}F resonances. Within each of the three areas, there are additional groups of resonances which arise from pentad structures and stereosequences, as will be discussed in detail below.

EEE Triads. In area A of Figure 3a, peaks 1–9 can be sorted into three groups along the ^{19}F dimension, with at least three peaks in each group. The three groups of peaks (peaks 1/4/7, peaks 2/5/8, and peaks 3/6/9) are the result of the three possible stereosequences rr, mr/rm, and mm for the EEE triads. The peaks

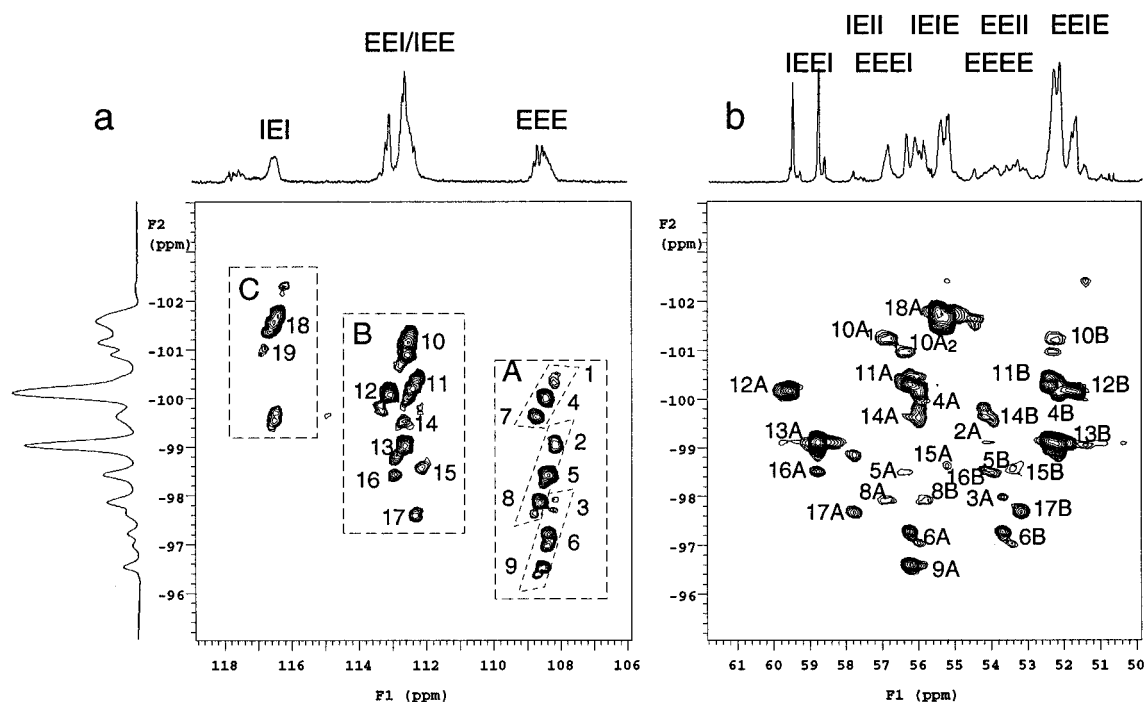


Figure 3. $^{19}\text{F}\{^{13}\text{C}\}$ HMQC spectrum (a) and HMBC spectrum (b) of P(CFE-IB) 3:1.

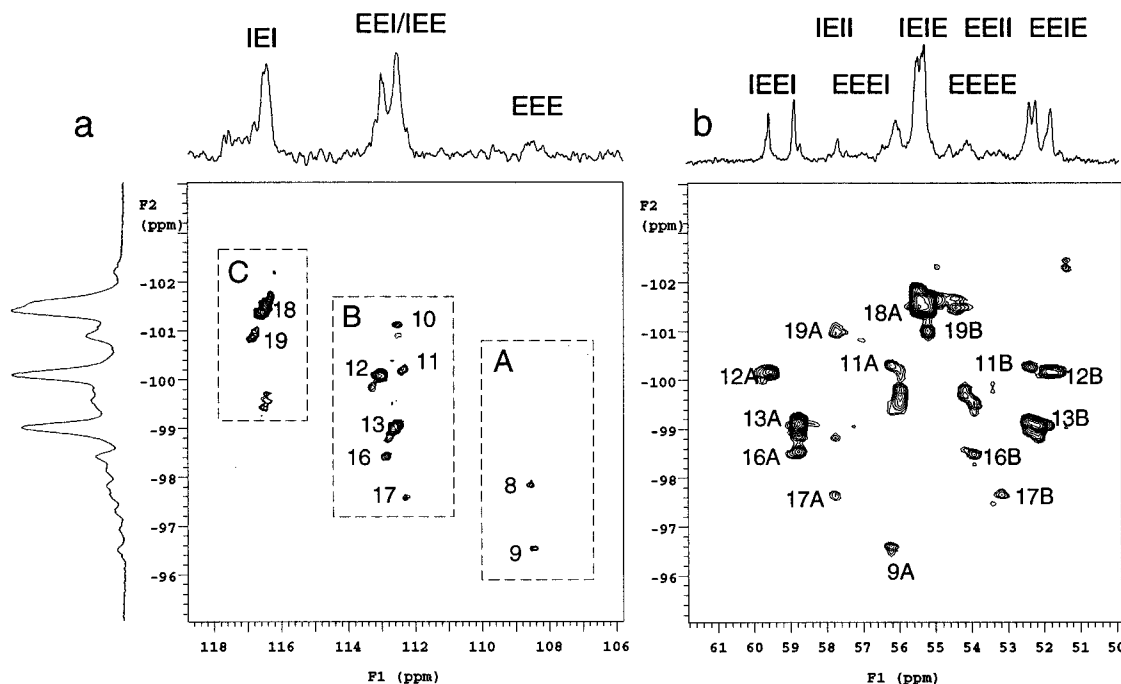


Figure 4. $^{19}\text{F}\{^{13}\text{C}\}$ HMQC spectrum (a) and HMBC spectrum (b) of P(CFE-IB) 1:1.

within each set are attributed to the sensitivity of the ^{19}F chemical shift to pentad structures. Cross-peaks 1, 2, and 3 are attributed to EEEEE pentads with rr, mr/rm, and mm stereosequences, respectively, by the comparison with the $^{19}\text{F}\{^{13}\text{C}\}$ HMQC spectrum of P(CFE) shown in Figure 5a.¹² Since the homopolymer peaks do not show further splitting due to stereosequence effects, the resonances in region A of Figure 3a must arise from additional monomer sequences which are possible if pentad structures are considered. Therefore, cross-peaks 4 and 7 are assigned to EEEEE and IEEEE pentads, respectively. Each replacement of an E with an I monomer unit in an EEEEE pentad to form EEEEE and IEEEE pentads results in a progressive 0.2 ppm downfield shift of the C–F ^{13}C resonance and a progressive 0.2 ppm downfield shift of the ^{19}F resonance.

Following this trend, the assignments of the rest of the peaks in this area could be made, and they are summarized in Table 1. Additional fine structures (e.g., doubling of peaks 3, 6, 8, and 9) may result from the sensitivity of ^{19}F shifts to heptad monomer sequences or to remote stereosequence effects.

The EEE triad region in the spectrum of P(CFE-IB) 1:1 (Figure 4a) only shows peaks 8 and 9, which confirms the above assignments. Sample P(CFE-IB) 1:1 has a much lower fraction of E units, so that the resonances from structures with more E units will have much lower relative intensity in the P(CFE-IB) 1:1 spectrum compared to the P(CFE-IB) 3:1 spectrum. Peaks 8 and 9 are from the IEEI pentad structure, which statistically should give more intense signals in

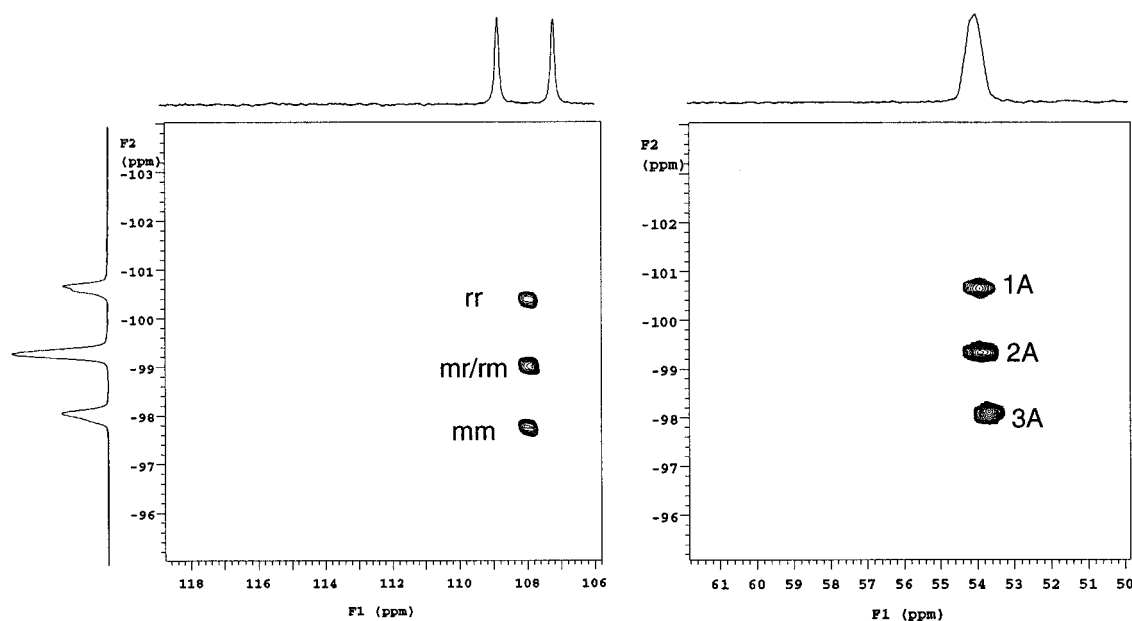


Figure 5. $^{19}\text{F}\{^{13}\text{C}\}$ HMQC spectrum (a) and HMBC spectrum (b) of P(CFE).

Table 1. Observed $^{19}\text{F}\{^{13}\text{C}\}$ HMQC and HMBC Correlations for $-\text{CF}(\text{Cl})\text{CH}_2-$ Groups

E-centered pentad	HMQC cross-peak	central triad stereosequence	$\delta_{19\text{F}}$ (ppm)	$\delta_{13\text{C}}$ (ppm) C-F	tetrads contained within pentad	HMBC cross-peak	$\delta_{13\text{C}}$ (ppm) CH_2
EEEE	1	rr	-100.3	108.2	EEEE	1A	54.0
	2	mr/rm	-99.0	108.1		2A	53.9
	3	mm	-97.9, -97.7 ^a	108.2		3A	53.7
EEEEI	4	rr	-100.0	108.5	EEEE/EEEEI	4B/4A	54.2/56.0
	5	mr/rm	-98.4	108.4		5B/5A	54.1/56.3
	6	mm	-97.2, -97.0 ^a	108.4		6B/6A	53.7/56.2
IEEEI	7	rr	-99.6	108.8	IEEE/EEEEI	7A	56.0
	8	mr/rm	-97.8, -97.6 ^a	108.6, 108.8 ^a		8A/8B	56.6/55.8
	9	mm	-96.5, -96.4 ^a	108.5, 108.7 ^a		9A	56.2
EEEIE	10	r	-101.2, -100.9 ^a	112.6	EEEE/EEEIE	10A/10B	56.6, 56.2 ^a /52.2
	11	m	-100.2	112.4		11A/11B	56.2/52.4
IEEIE	12	r	-100.1, -99.8 ^a	113.0, 113.3 ^a	IEEI/EEEIE	12A/12B	59.6/51.7
	13	m	-99.0, -98.8 ^a	112.6, 112.9 ^a		13A/13B	58.8/52.2
EEEII	14	r	-99.5	112.6	EEEE/EEII	14A/14B	56.0/54.1
	15	m	-98.6	112.1		15A/15B	55.2/53.4
IEEII	16	r	-98.4	112.9	IEEI/EEII	16A/16B	58.8/53.9
	17	m	-97.6	112.4		17A/17B	57.8/53.2
EIEIE	18		-101.7, -101.6 ^a	116.4, 116.5 ^a	IEIE	18A	55.4
EIEII	19		-101.0	116.8	EIEI/IEII	19B/19A	55.2/57.8
IEEII ^a	20		-100.4 ^b	117.7 ^b	IEEI/IEII		

^a Additional resonances are observed due to remote monomer and stereosequence effects. ^b Not observed but chemical shifts are estimated for completeness.

P(CFE-IB) 1:1 spectrum than in the P(CFE-IB) 3:1 spectrum.

EEI Triads. In area B of Figure 3a, eight major peaks are observed. Although the peak volumes in a 2D spectrum are related to the species concentrations, they are also dependent upon the relative J couplings and relaxation rates. Consequently, it may be possible to obtain qualitative information from peak volumes; however, quantitative interpretation of volume integrals is unreliable. By comparing the relative peak intensities in Figures 3a and 4a, these eight peaks can be grouped into four pairs, 10/11, 12/13, 14/15, and 16/17, with the peaks in each pair having similar intensities. The four groups result from different EEI-centered pentad structures (i.e., EEEIE, IEEIE, EEEII, and IEEII), and the two different peaks within each group are attributed to different stereosequences of the central triad (i.e., r and m). It should be noted that different configurations are possible for EE pairs but not for EI, IE, or II pairs. The much higher E content in the sample

used to obtain the spectrum in Figure 3a can be used to identify the resonances from pentad structures with higher E content.

Based on the above argument, cross-peaks 10 and 11 are assigned to EEEIE pentad structures with r and m stereochemical relationships for the central EEI triad, because they are the most intense peaks in Figure 3a but are significantly weaker in Figure 4a. Peaks 12 and 13 are the second most intense peaks in Figure 3a and are the most intense peaks in Figure 4a. Consequently, this pair of peaks arises from either EEEII or IEEIE pentads. Peaks 16 and 17 are more intense in Figure 4a, compared to Figure 3a. Thus they must arise from IEEII pentad structures with higher I content. The remaining pair of peaks (15/16) arises from either IEEIE or EEEII pentads. The assignments in this area are confirmed by the HMBC spectra which are described below.

IEI Triads. In the IEI triad region, three groups of resonances corresponding to EIEIE, EIEII, and IIEII

Table 2. Possible Methylene-Centered Tetrads Contained with E-Centered Pentad Sequences

pentad	related tetrads	pentad	related tetrads
EEEE	EEEE	EEEE	EEEE
EEEE	EEEE, EEIE	EEEE	EEEE
IEEE	EEEE	EIEE	EIEE
EEEE	EEEE, EEIE	EIEE	EIEE
IEEE	EEEE	EIEE	EIEE

pentad structures may be expected. Of these, resonances due to the IIEI pentad are not seen due to the statistically small amount of this pentad structure in the sample. In Figure 4a, three major resonances are found in area C. From area A, we notice that the ^{19}F chemical shift change due to a stereosequence difference is generally larger than the ^{19}F chemical shift change due to a monomer sequence difference. If the same effect is valid for the resonances from IEI-centered pentad structures, then the two upfield resonances (peaks 18 and 19) arise from different monomer sequences. The $^{19}\text{F}\{^{13}\text{C}\}$ HMBC spectrum must be examined before detailed assignments can be made for this area.

$2\text{D } ^{19}\text{F}\{^{13}\text{C}\}$ HMBC NMR Spectra. $^{19}\text{P}\{^{13}\text{C}\}$ HMBC spectra of P(CFE-IB) 3:1 and P(CFE-IB) 1:1 are shown in Figures 3b and 4b, respectively. These spectra exhibit correlations between ^{19}F resonances and ^{13}C resonances of methylene carbons which are two bonds away. The CH_2 signals from II-centered tetrad structures (EIII, EIII, and IIII) are not present in the spectra, since these methylene carbons do not have any two-bond J couplings to ^{19}F . Therefore, the resonances along the ^{13}C dimension are simplified compared to those in the $1\text{D } ^{13}\text{C}$ spectrum.

HMBC and HMBC spectra can be used in concert by matching ^{19}F signals from the C-F group in pentad structures that are observed in the HMQC spectrum with the cross-peaks of methylene ^{13}C resonances from tetrads in the HMBC spectrum. A slight chemical shift difference (ca. 0.1 ppm) can be observed between ^{19}F shifts in HMQC and HMBC spectra because of the one-bond ^{13}C isotope shift of the ^{19}F signals in the HMQC spectrum. To assist in the interpretation, the possible correlations between E-centered pentad and tetrad structures or between ^{19}F pentad resonances and ^{13}C resonances of adjacent CH_2 groups centered in various tetrads are listed in Table 2. For a symmetrical E-centered pentad structure, only one related CH_2 tetrad structure is present, and only one correlation of the ^{19}F resonance of such pentads to CH_2 tetrad resonances is possible. For example, the C-F in an IEEEE pentad can only be adjacent to a CH_2 in an EEEE tetrad. If the ^{19}F resonance position of an IEEEE pentad in the HMQC spectrum (Figure 3a, peak 9, or Figure 4a, peak 9) is related to a methylene resonance by a cross-peak in the HMBC spectrum (Figure 3b, peak 9A, or Figure 4b, peak 9A), the identity of the central methylene ^{13}C resonance in the EEEE tetrad can be determined.

A C-F centered in an asymmetric pentad such as IEEEE will be adjacent to two methylene groups. In this specific example, one will be centered in an EEEE tetrad, and the other will be centered in an EEEE tetrad. For example, the ^{19}F resonance position of an IEEEE pentad in the HMQC spectrum (Figure 3a, peak 6) is related to two methylene cross-peaks in the HMBC spectrum (Figure 3b, peaks 6A and 6B). Corresponding peaks are not found in the HMBC spectrum of P(CFE-IB)1:1 (Figure 4b), because the probability of having

an EEEEE pentad is much lower. Peak 6A can be assigned to a methylene in an EEEE tetrad, since its ^{13}C chemical shift is identical to that of peak 9A from the methylene tetrad within an IEEEE pentad. Consequently, peak 6B must arise from a methylene in an EEEE tetrad. Additional splitting of peaks 6A and 6B arises from hexad monomer sequences or further stereosequences.

By relating the ^{19}F resonance of the EEEEE pentad (Figure 3a, peak 3) with cross-peak 3A in the HMBC spectrum (Figure 3b), the ^{13}C resonances of the methylene group centered in an EEEE tetrad can be identified. Since resonance 3 is from a C-F within an EEEEE pentad, there can only be methylenes centered in an EEEE tetrad, and there is only a single cross-peak in the HMBC spectrum with the same ^{19}F chemical shift as cross-peak 3 in the HMQC spectrum. The ^{13}C shift of this methylene is nearly identical to that of cross-peak 6B, which also arises from a methylene within an EEEE tetrad. A similar argument applies to peak 2 in Figure 3a, which can be related to peak 2A in Figure 3b. The assignments of peaks 2A and 3A in Figure 3b are also confirmed by comparison with the HMBC spectrum of P(CFE), shown in Figure 5b.

There are two cross-peaks in the HMBC spectrum (8A and 8B) having ^{19}F shifts which are identical to that of peak 8 in the HMQC spectrum. Peak 8 arises from the C-F in an IEEEE pentad and therefore can only be attached to methylenes within EEEE tetrads; the two methylene resonances must result from stereosequence effects.

EEI-centered pentads which exhibit C-F correlations in region B of the HMQC spectrum (Figure 3a) can be joined to methylenes within four different types of tetrad sequences (EEEE, EEIE, IEEI, and EEII).

Although the peaks of the remaining pentad sequences can be found in the 2D-NMR spectra of both polymers, they are more clearly observed in the spectrum of P(CFE-IB) 1:1 (Figure 4a,b), which as the higher I content. Two pairs of peaks, 10A/10B and 11A/11B, are detected in the HMBC spectra corresponding to the EEI-centered ^{19}F pentad structures which produce peaks 10 and 11 (EEEE) in the HMQC spectrum. Peaks 10A and 11A are from methylenes in EEEE tetrad structures based on the correspondence of their ^{13}C chemical shifts with peaks 9A and 6A; thus peaks 10B and 11B must arise from CH_2 's centered in EEIE tetrads. Since peaks 12B and 13B appear in the same region as peaks 10B and 11B, they must also arise from EEIE tetrads. In this case, their related pentad structures, which produce peaks 12 and 13, must be from IEEIE sequences. Consequently, peaks 12A and 13A can be assigned to IEEI tetrads. Similar arguments can be applied to peaks 14 and 15; peaks 14A and 15A occur in the EEEE region, making EEEE their related pentad structure; therefore 14B and 15B are assigned to EEII tetrads. The remaining peaks (16 and 17) in region B of the HMQC spectrum in Figure 4a must arise from IEEI pentads. The methylene-centered tetrads associated with these pentads are IEEI and EEII. Cross-peaks 16A and 17A occur in the IEEI region of the HMBC spectrum, leaving cross-peaks 16B and 17B to be assigned to the methylene carbons in EEII tetrads, which match the assignments of 14B and 15B.

Many of the labeled cross-peaks exhibit additional broadening and/or splitting. These small differences in the shift within the same tetrad structure must arise from the different stereosequences.

In Figure 4b, cross-peaks 18A, 19A, and 19B are related to ^{19}F resonances in IEI-centered pentad structures. Since only one peak, 18A, corresponds to peak 18, it is assigned to the EIEI tetrad and is contained within EIEIE pentads. Two peaks, 19A and 19B, are found at the same ^{19}F shift of peak 19; thus the pentad structure must be EIEII. Cross-peak 19B occurs at the same ^{13}C shift as the EIEI tetrad resonance (18A); the remaining cross-peak, 19A, is therefore assigned to the IIEI tetrad. The resonance assignments for the methylene ^{13}C tetrad resonances are summarized in the last three columns of Table 1. It is evident from these entries that there are many overlapping ^{13}C methylene resonances from a specific tetrad sequence which are easily resolved due to dispersion of the ^{19}F resonances by monomer sequence and stereosequence effects. Two additional peaks in region C of Figure 3a (at $\delta_{19\text{F}} = -99.6$ and -102.3) cannot be attributed to any of the possible structures from the polymer backbone. These additional peaks might arise from defects in the polymer such as unsaturated monomer units or chain ends.

Conclusion

$^{19}\text{F}\{^{13}\text{C}\}$ HMQC and HMBC experiments are thus seen to be extremely useful for characterizing fluoropolymers, offering several advantages compared to their $^1\text{H}\{^{13}\text{C}\}$ counterparts. ^{19}F -containing copolymers exhibit complex peak patterns in the NMR spectra, due to stereosequence and monomer sequence distribution as well as couplings with ^{19}F . The $^{19}\text{F}\{^{13}\text{C}\}$ HMQC and HMBC experiments provide dispersed spectra by using both ^{13}C and ^{19}F large chemical shift ranges, and simplification of spectra is achieved by applying simultaneous ^1H decoupling. A phenomenal amount of information about complex polymer structures can be extracted from these spectra, despite the enormous number of possible monomer sequences and stereosequences. While it is possible that head-to-head structures might exist, the probability of forming such structures is small;¹³ no evidence for head-to-head structures was found in the data obtained in this work.

While in this paper $^1J_{\text{CF}}$ in HMQC and $^2J_{\text{CF}}$ in HMBC experiments are used to obtain information about C–F correlations, numerous other possibilities exist to obtain structural information which is not available in the corresponding C–H spin systems. The $^1J_{\text{CF}}$ and $^nJ_{\text{CF}}$ couplings are generally much larger than the corresponding $^1J_{\text{CH}}$ and $^nJ_{\text{CH}}$ couplings, making it possible to study polymers with broader lines using $^{19}\text{F}\{^{13}\text{C}\}$ HMBC experiments. $^1\text{H}\{^{13}\text{C}\}$ HMBC spectra of similar polymers have little or no cross-peak intensity because relaxation occurs during the long $1/(2 \times ^nJ_{\text{CH}})$ delay required to effect coherence transfer between ^{13}C and ^1H . Furthermore, the ranges of $^2J_{\text{CH}}$ and $^3J_{\text{CH}}$ overlap substantially (0–7 Hz), making it difficult to differenti-

ate between peaks arising through two- and three-bond connectivities. The ranges of $^1J_{\text{CF}} = 100\text{--}500$ Hz, $^2J_{\text{CF}} = 20\text{--}50$ Hz, $^3J_{\text{CF}} = 5\text{--}15$ Hz, and $^4J_{\text{CF}} = 0\text{--}5$ Hz are large and exhibit little overlap. It is therefore possible to obtain spectra with delays optimized for each of these coupling ranges and to use such spectra to unambiguously determine two-, three-, and sometimes four-bond connectivities, thus providing detailed information about numerous structure fragments.

Acknowledgment. We wish to acknowledge support from the National Science Foundation (Grant DMR-9310642), the Ohio Board of Regents Research Challenge Program, and The University of Akron Faculty Research Grant Program. We also wish to acknowledge the Kresge Foundation and donors to the Kresge Challenge Program at The University of Akron for funds used to purchase the 600 MHz instrument used in this work.

References and Notes

- (1) Muller, L. *J. Am. Chem. Soc.* **1979**, *101*, 4481.
- (2) Bax, A.; Griffey, R. G.; Hawkins, B. L. *J. Am. Chem. Soc.* **1983**, *105*, 7188.
- (3) Bax, A.; Summers, M. F. *J. Am. Chem. Soc.* **1986**, *108*, 2093.
- (4) Bax, A.; Morris, G. A. *J. Magn. Reson.* **1981**, *42*, 501.
- (5) Bax, A.; Morris, G. A. *J. Magn. Reson.* **1983**, *53*, 517.
- (6) Wilde, J. A.; Bolton, P. H. *J. Magn. Reson.* **1984**, *59*, 343.
- (7) (a) Rinaldi, P. L.; Li, L.; Hensley, D. R.; Ray III, D. G.; Harwood, H. J. *Macromol. Symp.* **1994**, *86*, 15. (b) Rinaldi, P. L.; Li, L.; Ray III, D. G.; Hatvany, G. S.; Wang, H. T.; Harwood, H. J. In *Multidimensional Spectroscopy of Polymers*; ACS Symposium Series 598; Urban, M. W., Provder, T., Eds.; American Chemical Society: Washington, DC, 1995; p 213.
- (8) Majumdar, R. N.; Harwood, H. J. *Applied Polymer Analysis and Characterization*; Mitchell, S., Jr., Ed.; Hansen: New York, 1987; p 423.
- (9) States, D. J.; Haberkorn, R. A.; Ruben, D. J. *J. Magn. Reson.* **1982**, *48*, 286.
- (10) Garbow, J. R.; Weitekamp, D. P.; Pines, A. *Chem. Phys. Lett.* **1982**, *93*, 504.
- (11) The relative shifts of C–F resonances from EEE, EEI, and IEI triads are based in part on the statistical probability of their formation and the relative intensities of resonances in the 108–117 ppm region of the ^{13}C spectra obtained from polymers prepared with 3:1 and 1:1 E:I monomer feed ratios. Further evidence for the proposed assignments is obtained from HMQC and HMBC spectra which are presented below.
- (12) The assignment of resonances from P(CFE) to mm, mr/rm, and rr stereosequences had been made based on 3D-NMR experiments which have permitted detection of individual methylene ^1H resonances and relation of these resonances to ^{19}F and ^{13}C resonances from atoms which are one- or two-bonds removed. Methylene protons in r diads are essentially chemically equivalent and those in m diads are nonequivalent; therefore carbons which are directly bound to non-equivalent protons are located in m diads. These results are being reported elsewhere.
- (13) (a) Moad, G.; Solomon, D. H. *Free Radical Polymers*; Elsevier: New York, 1995; pp 8–11. (b) *Ibid.*, pp 152–159.

MA9600015